A Numerical Study on Strut-Placed Supersonic Flow in Annulus Flowfield

Hee Jun Park[*1], Won Goo Joo[2]

스트럿트가 있는 초음속 환형유동장에 대한 수치적 연구

박희준, 주원구

In this numerical approach, strut-placed supersonic annular flow is examined. The geometrical variations of strut cause strong influence on flowfield structures. The geometrical variations are as follows ; swept effect, attack angle effect, variation of leading edge shape. These changed features such as velocity structure, pressure structure, shock-boundary layer interaction are compared and analyzed according to each geometrical configuration.

Key Words: supersonic annular flowfield(초음속 환형유동장), shock-boundary layer interaction(경계층-충격파 간섭), secondary shock-expansion wave structure (이차 충격파-팽창파 구조), Boundary layer thickness(경계층 두께), swept effect(쏠림효과)

1. Introduction

The supersonic annular flowfield with vanes is an important subject of engineering application. Especially, the accurate analysis of supersonic flowfield becomes an important issue of the application such as high speed vehicle, propulsion. In this numerical study, the variation of flowfield structure is examined according to geometrical variation of strut. The incoming supersonic flow interacts with vane structure and shock and expansion wave are developed. These induced shock wave structures interact with boundary wall. As a result, very complex flow structures are produced. The geometrical variations of strut are as follows; swept effect, attack angle variation, leading edge shape variation. At each geometrical configuration, the resulting flow structure show different features in velocity, pressure field, shock-expansion wave, shock-boundary layer interaction.

[*1]KIST
[2]연세대학교 기계공학과 대학원

2. Numerical method

2.1 Governing Equation

In this numerical approach, supersonic annular flowfield is characterized by compressibility, steady state and integral time-averaged cylindrical coordination is applied as a governing equation.

Continuity Equation :

$$\frac{\partial}{\partial t}\oint_{VOL}\rho\ dVOL+\oint\rho\ \bar{q}d\overline{AREA}=0 \quad (1)$$

Momentum Equation :

$$\frac{\partial}{\partial t}\oint_{VOL}\bar{U}\,dVOL+\oint\rho\ \overline{H}\,d\overline{AREA}=\oint\rho\bar{S}\,dVOL \quad (2)$$

$$\bar{U}=\begin{vmatrix} W_x \\ r\rho\ W_\theta \\ \rho\ W_r \end{vmatrix} \quad (3),\qquad \bar{H}=\begin{vmatrix} \rho\ W_x\bar{q}+\bar{\tau}i_x \\ r\rho\ W_\theta\bar{q}+\bar{\tau}i_\theta \\ \rho\ W_r\bar{q}+\bar{\tau}i_r \end{vmatrix} \quad (4)$$

$$\bar{S}=\begin{vmatrix} 0 \\ -2\Omega r W_r \\ \frac{W_\theta^2}{r}+r\Omega^2+2\Omega W_\theta \end{vmatrix} \quad (5)$$

Here, $\bar{q}=W_x i_x+W_r i_r+W_\theta i_\theta$ (6)

Eq.(6) stands for relative velocity vector and Ω represents angular velocity and $\bar{\tau}$ is stress tensor which include both shear stress and pressure component.

Energy Equation :

$$\frac{\partial}{\partial t}\oint_{VOL}\rho E\,dVOL+\oint\rho I\bar{q}\,d\overline{AREA}=0 \quad (7)$$

Here, E is specific energy and I is Rothalpy which is defined as $I=c_pT_{0rel}-\frac{1}{2}(\Omega r)^2$ (8)

and here T_{0rel} is relative total temperature.

Ideal Gas Equation :

$$p=\rho(\gamma-1)(E-0.5*(\bar{q}\cdot\bar{q}-(\Omega r)^2)) \quad (9)$$

2.2 Numerical Procedure

In order to apply governing equation to physical domain, governing equations are transformed to body fitted coordination and integrated by finite volume method. Convection term and diffusion term are discretized by central differencing scheme and artificial dissipation is used to resolve numerical dispersion problem and facilitate shock capturing. Baldwin-Lomax turbulence model is used.

On the basis of the characteristic theory, boundary conditions are assigned as follows ; At inlet boundary, all flow variables are fixed(Dirichlet Condition). At exit boundary, all flow variables are extrapolated. At wall boundary, no slip condition and adiabatic condition are applied.

2.3 Test section and specification[1]

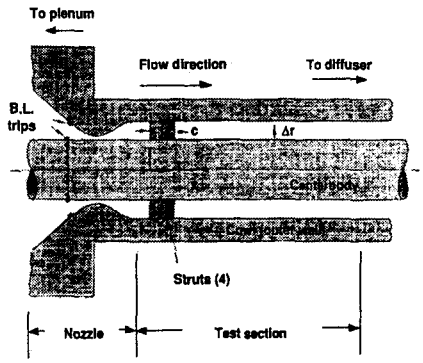

Fig. 1 Schematic of test section

In Fig. 1, a schematic of test section is shown. It is composed of cowl(outer wall) and centerbody(inner wall) which have constant cross section area and four struts of diamond shape are attached to cowl at 90° intervals.

item	size
centerbody diameter	83.0 mm
cowl diameter	118.6 mm
constant annular gap	17.8 mm
strut height	17.8 mm
midchord width	25.4 mm
maximum strut thickness	3.18 mm

Table. 1 Geometry specification

3. Numerical Results and analysis of Unswept strut and Swept strut

3.1 Grid Generation and Computational Domain

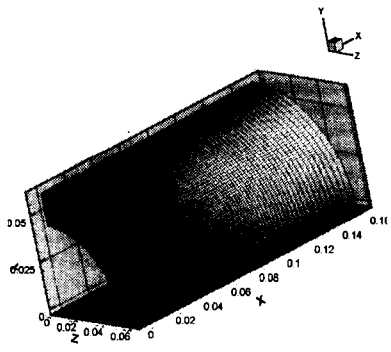

Fig. 2 Computational domain

In Fig. 2, computational domain is shown. Because this supersonic annular flowfield is axisymmetrical flow, one passage is calculated. A 135*75*151(x-r-θ) grid is used for the discretization of the flow domain.

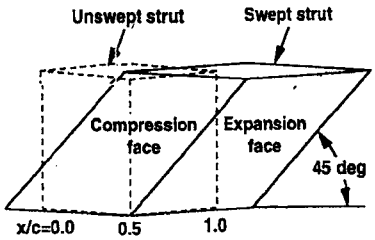

Fig. 3 Schematic of strut configuration

In Fig. 3, a schematic of strut is shown. As shown in Fig. 3, at swept strut, leading edge and trailing edge are inclined toward downstream direction by 45° .

3.2 Boundary condition

Inlet boundary condition is as follows ; Mach No. : 2.9, total pressure : 1034 mm Hg, total temperature : 297.15K.

At exit boundary condition, all flow variables are extrapolated.

3.3 Numerical results and analysis

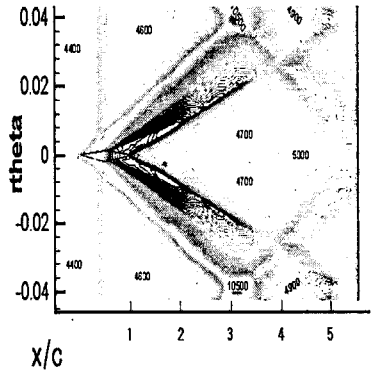

(a) unswept strut

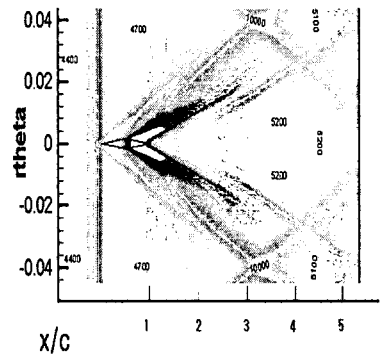

(b) swept strut

Fig. 4 Pressure contour at midspan plane

In Fig. 4, pressure contour at midspan plane is shown. By the comparison between Fig. 4 (a) and (b), the effect of swept strut on pressure field can be examined. In case of unswept strut, because shock wave is normal to cowl and centerbody, the position of shock wave is constant along the axis direction. On the other hand, in case of swept strut, shock wave is inclined relative to cowl and center body. Therefore, the position of shock wave is more downstream, as a position approaches cowl. This shock structure causes ununiformity of velocity and pressure field structure relative to radial direction. In regard to the points through which shock wave passes, the flow which is located above the points in radial direction is not affected by shock wave and the flow which is located below the points in radial direction is affected by shock wave. Therefore, the difference in pressure and velocity between two flow areas becomes larger. By this influence of ununiformity, the strength of shock-expansion structure is weakened at swept strut.

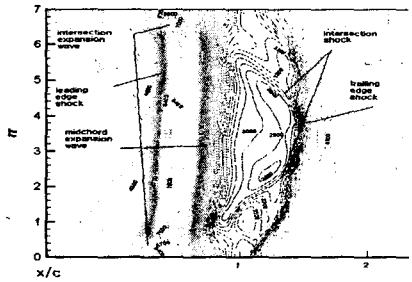

(a) unswept strut

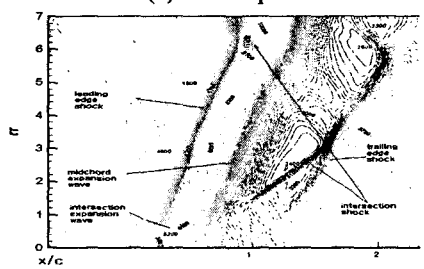

(b) swept strut

Fig. 5 Secondary shock structure at at meridional plane

In Fig. 5, the pressure contour at meridional plane at near strut region is shown. The shock-expansion wave structures which are produced at leading edge, midchord, trailing edge interact with wall boundary and secondary shock-expansion wave structures are formed.

In general, the feature of secondary shock-expansion wave structure depends on geometry of wall boundary. In case of unswept strut, oblique shock at leading edge interacts with wall and produce secondary expansion wave. Expansion wave at midchord interacts with wall and produces secondary shock wave.

On the other hand, in case of swept strut, oblique shock at leading edge which interacts with wall of cowl produces secondary strong shock wave. By the swept effect, the secondary shock-expansion wave structures are changed and these changes affect the pressure and velocity field at near wall region. For example, because secondary shock wave makes pressure get larger in the direction of wall, flow at near wall region moves toward midspan area. In case of secondary expansion wave, flow at near wall region moves toward wall.[2]

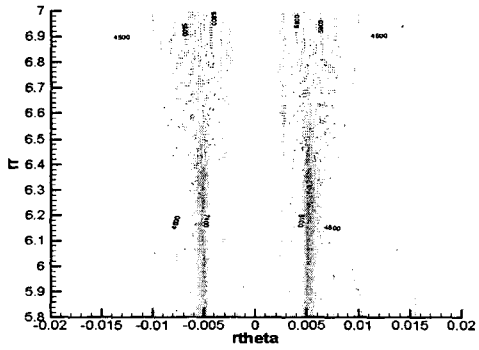

(a) unswept strut near cowl

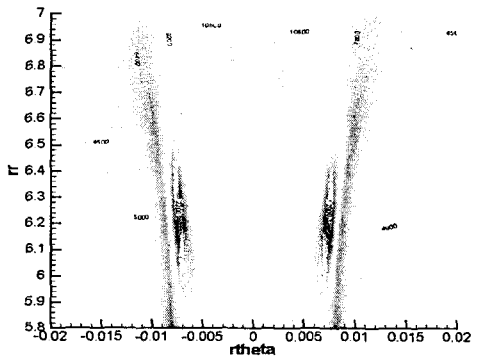

(b) swept strut near cowl

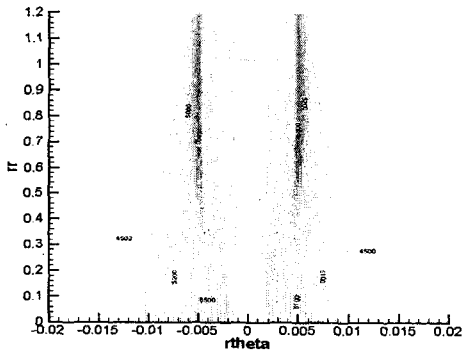

(c) Unswept strut near centerbody

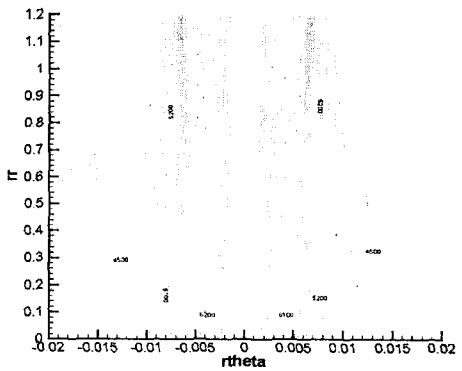

(d) swept strut near centerbody

Fig. 6 Pressure contour at x/c=0.85

In Fig. 6, pressure contour at x/c=0.85 is shown. (Here C is chord length) By the comparison of pressure distribution, the intensity of shock-boundary interaction can be analyzed. Swept effect have a strong influence on the strength of shock-boundary layer interaction. In general, inlet mach number and strut wedge angle are chief factor which play an important role in the strength of shock-boundary interaction. However, in the case of the same mach number and strut wedge angle, swept effect can be dominant factor in affecting shock-boundary interaction. By the analyses of the numerical results, following results can be summarized. If shock has acute angle with main stream, the strength of shock-boundary layer interaction becomes high. This is the case with swept strut near cowl(Fig 6. (b)). If shock has right angle with main stream, the strength of shock-boundary layer interaction becomes modest. This is the case with unswept strut(Fig 6. (a), (c)). If shock has obtuse angle with main stream, the strength of shock-boundary layer interaction becomes weak. This is the case with swept strut near centerbody(Fig 6. (d))

4. Numerical Results and analysis of Unswept strut according to variation of attack angle

4.1 Grid Generation and Boundary Condition

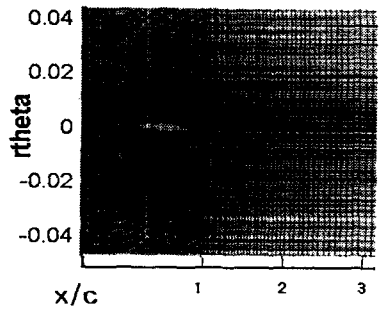

(a) attack angle 5°

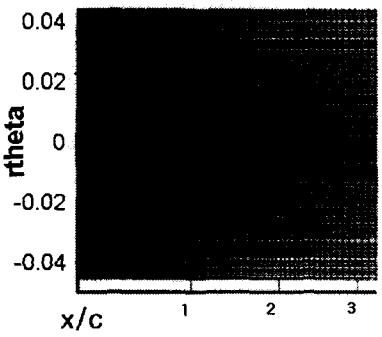

(b) attack angle 10°

Fig. 7 The schematic of strut configurations

In Fig.7, the schematic of unswept strut configurations according to each attack angle variation (5° , 10°) are shown.

The shape and specification of test section, computational grid and boundary condition are the same as chapter 3.

4.2 Numerical results and analysis

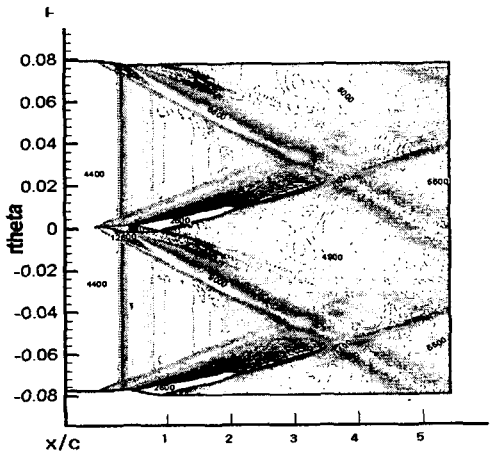

(a) attack angle 5°

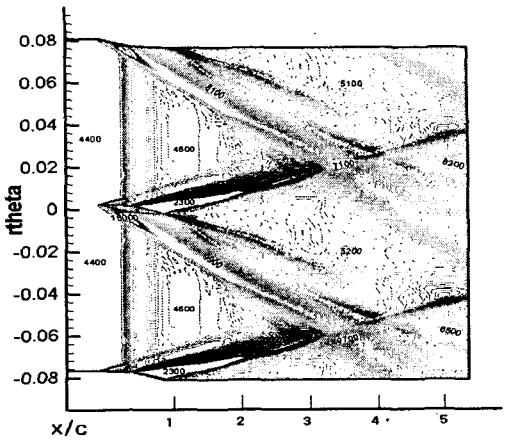

(b) attack angle 10°

Fig. 8 Pressure contour at midspan plane

In Fig. 8, pressure contour at midspan plane is shown. As shown at Fig 4. in the case of attack angle 0° , the distribution of pressure field is symmetrical with respect to strut. However, As attack angle of leading edge becomes larger, the intensity of asymmetry gets larger.

The half wedge angle of strut is 7.1° . In the case of attack angle 5° , at the positive circumferential direction, weak oblique shock is produced at leading edge and expansion wave is produced at midchord. At the negative circumferential direction, In the case of attack angle 10° . strong oblique shock is produced at leading edge and expansion wave is produced at midchord.

In the case of attack angle 10° , at the positive circumferential direction, expansion wave is produced at both leading edge and midchord. At the negative circumferential direction, strong oblique shock is produced at leading edge and expansion wave is produced at midchord.

As shown above, asymmetry of pressure field is intensified by the attack angle increase. Because the asymmetry caused by attack angle variation cause a strong influence on pressure, velocity, temperature field, these factors should be

considered at the design of engineering application such as high velocity vehicle, propulsion.

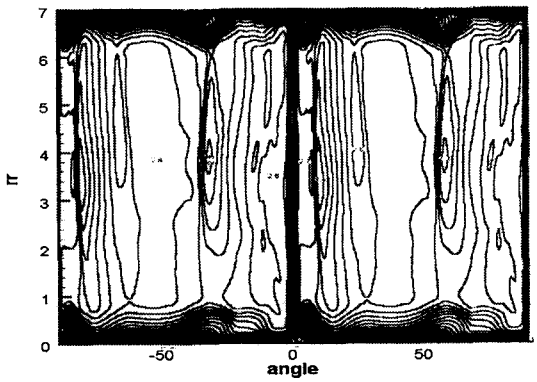

(a) attack angle 5°

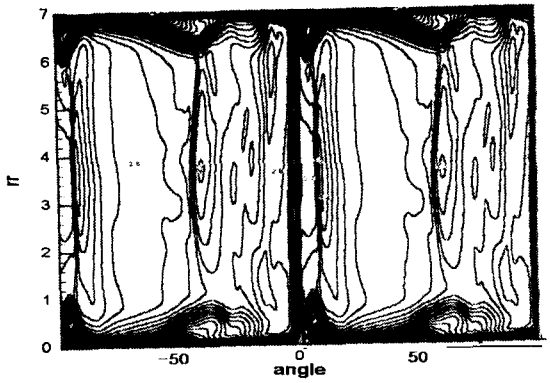

(b) attack angle 10°

Fig. 9 Mach number contour at x/c=2

In Fig. 9, mach number contour at x/c=2 is shown. In the region of flow with high momentum, boundary layer thickness becomes smaller, On the contrary, in the region of flow with low momentum boundary layer thickness becomes larger.

By the asymmetry caused by attack angle increase, strong velocity, pressure gradient is produced and these gradients cause instability of boundary layer.

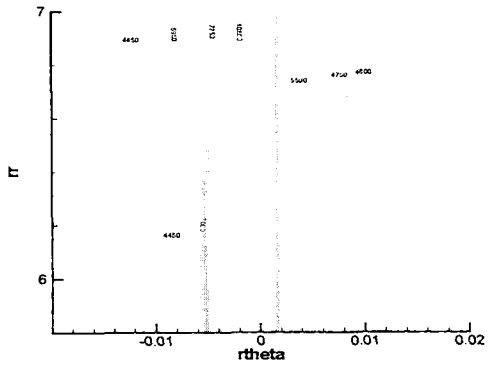

(a) attack angle 5° near cowl

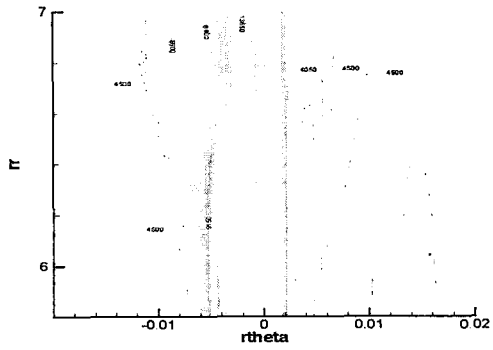

(b) attack angle 10° near cowl

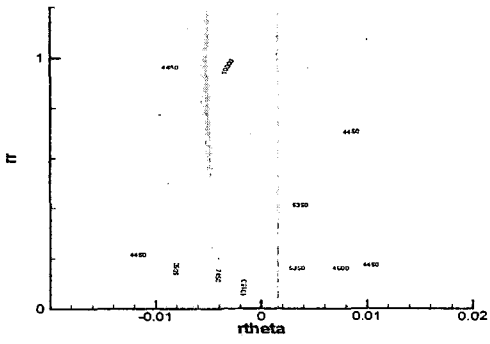

(c) attack angle 5° near centerbody

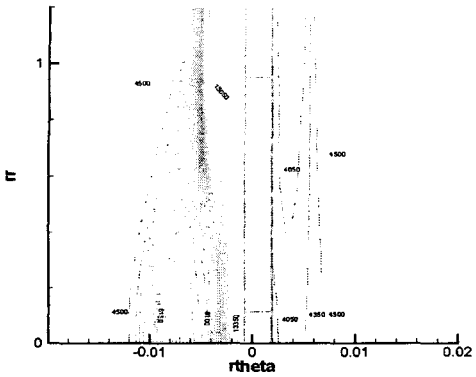

(d) attack angle 10° near centerbody

Fig. 10 Pressure contour at x/c=0.85

In Fig. 10, pressure contour at x/c=0.85 is shown. By the comparison among pressure countour at near various wall conditions, following results are summarized. The intensity of shock-boundary interaction is larger at the high attack angle and cowl region

5. Numerical Results and analysis of Unswept strut according to variation of leading edge feature(sharp versus round)

5.1 Schematic of strut, Grid Generation and Boundary Condition

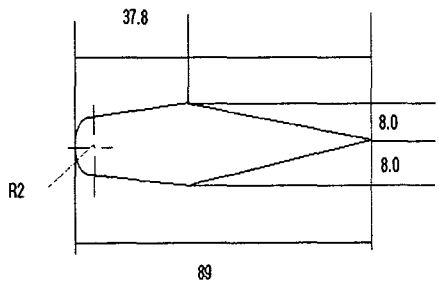

(a) Over view

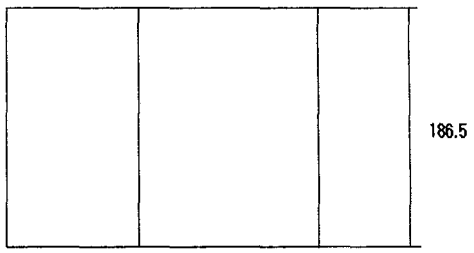

(b) Side view

Fig. 11 Round strut configuration

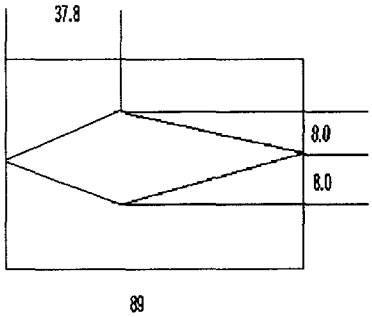

(a) Over view

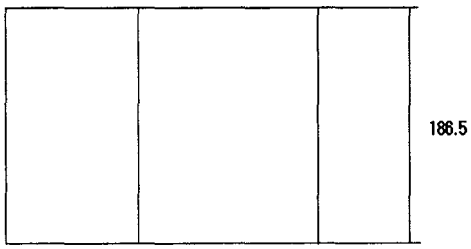

(b) Side view

Fig. 11 Sharp strut configuration

In Fig. 11, Round and sharp strut configuration are shown. Boundary condition are as follows; Inlet boundary condition is as follows ; Mach No. : 2, total pressure : 1034 mm Hg, total temperature : 297.15K.

At exit boundary condition, all flow variables are extrapolated.

A 255*75*151(x-r-θ) grid is used for the discretization of the flow domain.

5.2 Numerical results and analysis

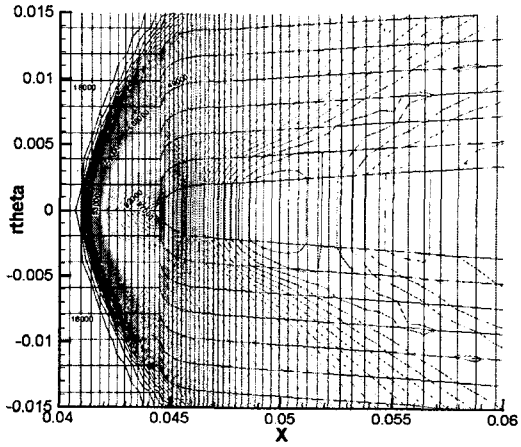

(a) Round strut

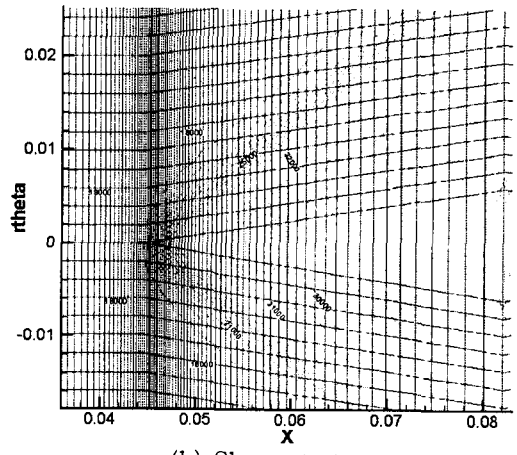

(b) Sharp strut

Fig. 12 Pressure contour at midspan plane near leading edge

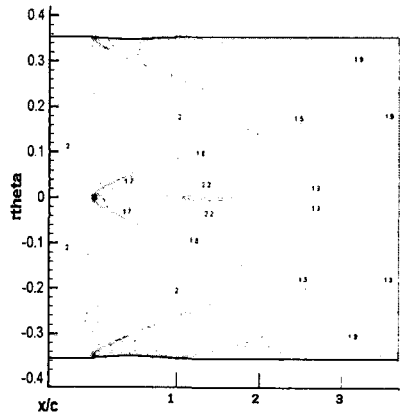

(a) Round strut

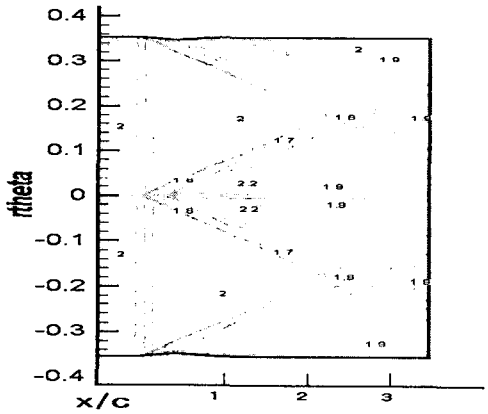

(b) Sharp strut

Fig. 13 Mach number contour contour at midspan plane

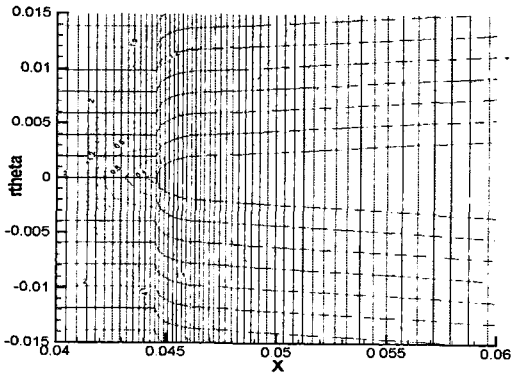

(a) Round strut

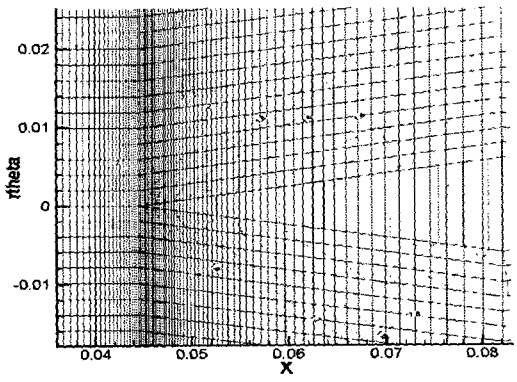

(b) Sharp strut

Fig. 14 Mach number contour contour at midspan plane near leading edge

From the analyses from Fig. 12, to Fig. 14, following results can be summarized.

By difference between characteristics of the detached shock and attached shock, resulting velocity, temperature, pressure field are developed in different ways. For example, normal shock caused by detached shock induces very high pressure and temperature region in front of leading edge. In the case of this numerical results, the peak pressure value of round strut is three times as large as that of sharp strut. By the normal shock effect, low momentum area(subsonic flow) is formed at near upstream of leading edge and this low momentum flow propagates downstream. Therefore, low momentum flow is produced at downstream of round strut. However, in the faraway region from the strut in circumferential direction, by the weak shock wave or mach wave, relatively high momentum flow is developed.

6. Conclusion

By the comparison and analysis among each numerical result of strut configuration, the influence of geometrical effect on flowfield structure is examined.

By the swept effect, the intensity of shock-expansion wave structure of swept strut is weaker than that of unswept strut and secondary shock-expansion wave structure is changed. As a result, flow streamlines near wall are different from that of unswept strut. On the other hand, because the angle shock has with main stream is changed by swept effect(namely, acute or obtuse angle), the intensity of shock-boundary layer interaction is also changed. In case that shock has acute angle with main stream, shock-boundary layer interaction strength becomes higher. On the contrary, in case that shock has obtuse angle with main stream, shock-boundary layer interaction strength becomes lower.

As attack angle is increased, in the circumferential direction, asymmetric flowfield structure are developed more intensively. Therefore, very high dynamic, thermal gradient is developed around strut and boundary layer can be unstabilized.

By the asymmetric flowfield, shock-boundary layer interaction becomes asymmetric. In the positive circumferential direction, weak shock and intensive expansion wave are developed. Therefore, the strength of shock-boundary layer interaction is decreased. On the other hand, in the negative circumferential direction, intensive shock is developed and intensive shock-boundary layer interaction is formed. These phenomena cause a strong thermal, dynamic load in the local region. Therefore, this factor should be considered at the design of engineering application.

In order to resolve ablation problem of vanes, the shape of leading edge is often designed in the form of blunt body. But, detached shock caused by blunt body, causes a strong influence on flowfield structure. Normal shock caused by detached shock brings out very high pressure, temperature region with

low momentum(subsonic region) in front of leading edge. This region induces a strong dynamic, thermal load and low momentum region at the downstream of strut which has low degree of momentum and heat transfer. On the contrary, in the faraway region from the strut in circumferential direction, relatively high momentum flow is developed.

As shown above, by the geometrical variation of strut, we can influence on flowfield in various ways. In the engineering application related to change of vane geometry, it is helpful to understand each effect of geometry factor of vane in achieving more effective and well-controlled results.

7. Reference

[1] K. E. Williams and F. B. Gessner "Flowfield Characteristics of Struts in Supersonic Annular Flow", Experimental Thermal and Fluid Science, 17, 1998, pp 156-164

[2] K. E. Williams and F. B. Gessner "Flowfield Characteristics of Swept Struts in Supersonic Annular Flow", Experimental Thermal and Fluid Science, 21, 2000, pp 278-284